AIAA JOURNAL
Vol. 60, No. 4, April 2022



# Technical Notes

## Fuel Regulation Historical Effects on Flame Stabilizations in a Cavity-Based Scramjet Combustor

Xu Zhang,* Qifan Zhang,† Zhenjie Wu,‡ Lianjie Yue,§ Zhanbiao Gao,¶ Weihang Luo,** and Hao Chen††
*State Key Laboratory of High Temperature Gas Dynamics, Institute of Mechanics, Chinese Academy of Sciences, 100190 Beijing, People's Republic of China*

https://doi.org/10.2514/1.J061306



### I. Introduction

DUAL-MODE scramjet engines are practical hypersonic air-breathing propulsions. Dual-mode traditionally means that a combustor can operate in the ramjet mode (the minimum Mach number $Ma_{\min} < 1.0$) or the scramjet mode ($Ma_{\min} > 1.0$) assuming 1-D flows [1,2]. As combustor inflows are supersonic, cavities are commonly used to stabilize flames. Two flame stabilization locations are generally observed in cavity-based combustors with upstream fuel injections [3–6]. They are named as the jet-wake stabilized mode and the cavity stabilized mode [3], in which the flame fronts are upstream and downstream of the cavity fore-walls, respectively. Combustion hystereses were observed by previous researchers [1,2,7–11], showing wall pressures depending on historical regulation directions of fuel equivalence ratio (ER). Mathematically, hysteresis originates from multisolution combustion states, and transitions between different states usually cause sudden changes mentioned as catastrophes. In the multisolution region, the real combustion state depends on the historical ER regulation path. Previous studies explained the multiple solutions of combustion states as the ramjet/scramjet modes by 1-D flow analyses [7–11], and meanwhile, historical ER regulation direction was the only historical path parameter considered. From the view of flame structures, our former studies [1,2] further certified that the multiple solutions could be the aforementioned flame stabilization modes. Multiple solutions and catastrophes of thrusts coming with hysteresis will make flight control difficult, and thus a deeper study of the historical path effects of ER regulations on flame stabilizations is essential.

This Note focuses on the historical path effects of ER regulations on flame stabilizations. Direct-connect tests of a cavity-based ethylene-fueled scramjet combustor were conducted. The air inflow was Mach 2.5 at a stagnation temperature of 1224 K. Different historical ER regulation path parameters, including initial values, regulation directions, and regulation rates, were investigated. Wall pressures and thrusts were measured, and flame/shock images were captured by high-speed photography of shadowgraph and CH* chemiluminescence.

### II. Experimental Setup

Experiments of a test-section scramjet combustor were performed using a direct-connect test facility in the Institute of Mechanics, Chinese Academy of Sciences. The facility used a $H_2-O_2-$air combustion heater and a Laval nozzle to provide test-section inflows. Figure 1 displays the test-section model containing a constant-area isolator and an expansive duct with cavity flame holders. The model was constantly 80 mm wide, and its inlet was 40 mm high. Ethylene fuel and pilot hydrogen were injected through wall-normal sonic orifices. There were nine ethylene injection orifices of diameter 1.0 mm and six hydrogen injection orifices of diameter 0.7 mm on the upper and lower walls, respectively. Pilot hydrogen was used to generate pilot flame for the ignition assistance of the ethylene fuel, and its injection stopped once the ethylene was ignited. Pilot hydrogen ER was around 0.05 and ethylene ER differed in each test. Multiple measurements were used, including wall pressures, thrusts, and high-speed photography of shadowgraph and CH* chemiluminescence. Wall-pressure measuring ports were marked as $p_1-p_{19}$ along the streamwise direction $x$. The shadowgraph observation region was around the injectors for shock/flow separation visualizations. CH* chemiluminescence was a marker of ethylene-fueled heat release intensity [12], and the observation region was around the cavities to observe flame stabilizations. More details of the facility, test-section model, and measuring methods can be found in a prior study [2].

The test-section inflow was constant, simulating a flight Mach number $Ma_f = 5$ at 27 km altitude. The inflow parameters are listed in Table 1. The inflow Mach number $Ma_{\text{in}}$, stagnation temperature $T^*_{\text{in}}$, and stagnation pressure $p^*_{\text{in}}$ were 2.5, 1224 K, and 1500 kPa, respectively. The relevant inflow temperature $T_{\text{in}}$ was 555 K. Hereinbelow, the reference pressure $p_{\text{ref}}$ for wall-pressure normalizations equals the inflow static pressure $p_{\text{in}}$ of 75 kPa.

Experiments were performed using the following scheme. First, the effects of historical ER variation directions of ethylene fuel on combustion states were studied by multistep ER regulations, as displayed in Fig. 2. The red and black lines represent historical decreasing and increasing of ER to the same target value, respectively. Referring to the former studies [1,2] of hysteresis associated with flame stabilization mode transitions, the initial ER should satisfy certain requirements. Specifically, the initial flame should be in the jet-wake stabilized mode if the ER was historically decreasing. Otherwise, it should be in the cavity shear-layer stabilized mode. By this scheme, tests of multiple target ERs were conducted to obtain traditional combustion hysteresis depending only on historical ER variation directions. Then, by using the multistep ER regulation paths, more tests were performed to study the effects of other historical ER regulation parameters, including initial values and

Received 22 September 2021; revision received 3 December 2021; accepted for publication 19 January 2022; published online 15 February 2022. 

*Postdoctoral Researcher, State Key Laboratory of High-Temperature Gas Dynamics, Institute of Mechanics; also School of Engineering Science, University of Chinese Academy of Sciences, 100049 Beijing, People's Republic of China.

†Research Assistant, State Key Laboratory of High-Temperature Gas Dynamics, Institute of Mechanics; zhangqifan@imech.ac.cn (Corresponding Author).

‡Ph.D. Candidate, State Key Laboratory of High-Temperature Gas Dynamics, Institute of Mechanics; also School of Engineering Science, University of Chinese Academy of Sciences, 100049 Beijing, People's Republic of China.

§Professor, State Key Laboratory of High-Temperature Gas Dynamics, Institute of Mechanics; also School of Engineering Science, University of Chinese Academy of Sciences, 100049 Beijing, People's Republic of China. yuelj@imech.ac.cn (Corresponding Author).

¶Intermediate Engineer, State Key Laboratory of High-Temperature Gas Dynamics, Institute of Mechanics.

**Junior Engineer, State Key Laboratory of High-Temperature Gas Dynamics, Institute of Mechanics.

††Research Assistant, State Key Laboratory of High-Temperature Gas Dynamics, Institute of Mechanics.

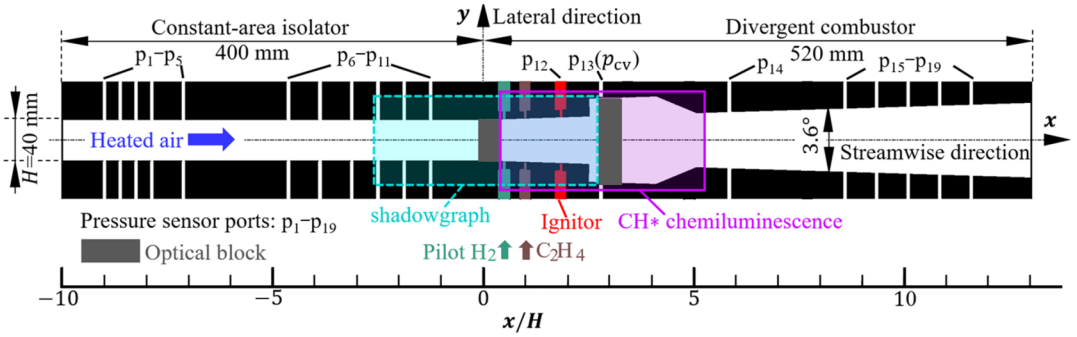


**Fig. 1 Schematic diagram of the scramjet combustor.**

**Table 1 Test-section inflow condition**

| $Ma_{in}$ | $T^*_{in}$, K | $p^*_{in}$, kPa | $T_{in}$, K | $p_{in}$, kPa |
|---|---|---|---|---|
| 2.5 | 1224 | 1500 | 555 | 75 |

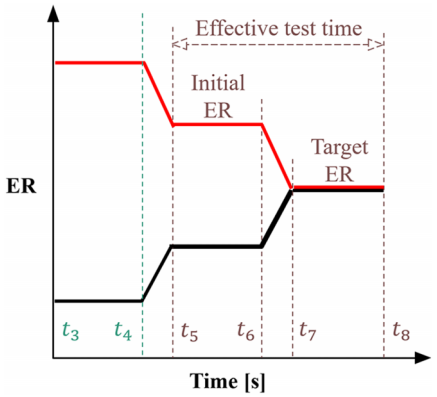


**Fig. 2 Schematic of ER regulation paths.**

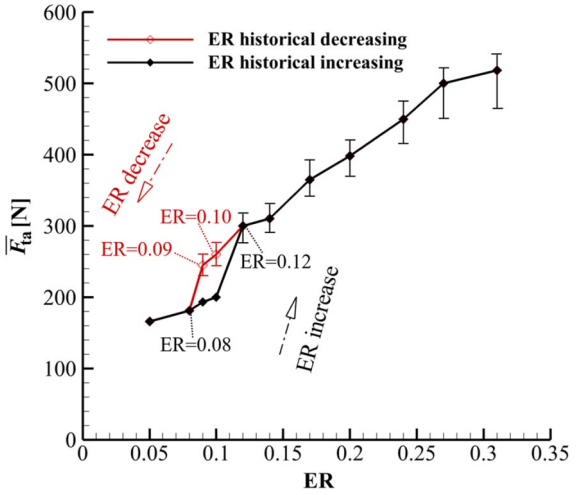


**Fig. 3 Time-averaged thrust $\overline{F_{ta}}$ vs target ER conditions. Diamond symbols represent $\overline{F_{ta}}$, and short horizontal lines represent the oscillation limits.**

historical decreasing/increasing rates. When one parameter was studied by contrast tests, the other parameters should be consistent.

## III. Results and Discussion

Focusing on the effects of historical ER variation directions, the following Sec. III.A illustrates a combustion hysteresis loop associated with dual-solution states showing as the two flame stabilization modes. Then effects of more historical ER regulation parameters were taken into considerations. Taking cases of certain target ER in the dual-solution region as examples, Sec. III.B illustrates the historical effects of ER initial values and decreasing rates on flame stabilizations. Subsequently, the reasons for historical ER regulation effects are speculated in Sec. III.C.

### A. Hysteresis Associated with Two Flame Stabilization Modes

Thrust, which commonly means thrust augmentation in ground tests, is of interest. It is defined as the measured thrust augmentation of the test section in the case at a certain target ER compared with the case with no fuel injection [2]. Figure 3 displays the time-averaged thrust $\overline{F_{ta}}$ versus target ER conditions. The diamond symbols represent $\overline{F_{ta}}$, and the short horizontal lines represent thrust oscillation limits. This chart illustrates a hysteresis loop in the ER range of 0.08–0.12. For a target ER = 0.09 or 0.10 in this range, $\overline{F_{ta}}$ had two potential solutions depending on historical ER regulation directions, and was obviously larger in the historical ER decreasing path. Moreover, thrust oscillations were obvious at the higher thrust branch, but ignorable at the lower thrust branch. These results indicate different types of combustion states in the dual-solution ER range. The slope changes in $\overline{F_{ta}}$ versus ER across this range indicated thrust catastrophes. Outside the dual-solution range, $\overline{F_{ta}}$ varied smoothly at different ERs without catastrophe.

Figure 3 indicates two different combustion flow states in the dual-solution region. According to shadowgraph and CH* chemiluminescence data, the dual-solution states were confirmed as two flame stabilization modes. Figure 4 presents typical shadowgraph and CH* chemiluminescence images at ER = 0.09 showing the two modes. Green-dashed and yellow-dashed lines in the images mark injection bow shocks and precombustion shocks, respectively. CH* chemiluminescence pseudocolors with a color bar normalized between 0 and 1 illustrate heat release intensities. Figure 4a displays the jet-wake stabilized mode corresponding to the higher-pressure branch at ER = 0.09 in Fig. 3. The flame front was upstream of the cavities, along with precombustion shocks indicating flow separation upstream of the cavities. Figure 4b displays the cavity shear-layer stabilized mode corresponding to the lower-pressure branch at ER = 0.09. The flame was downstream of the cavities and mostly near the cavity aft-walls. Furthermore, no precombustion shock in view indicated that the flow was mainly supersonic without separation.

### B. Historical Effects of ER Initial Values and Decreasing Rates on Flame Stabilizations

For a target ER = 0.09 in the dual-solution region illustrated in above Fig. 3, the flame should be in the jet-wake stabilized mode in the historical ER decreasing path. To explore whether initial ER values would historically affect flame stabilizations in the historical ER decreasing path, three tests with different initial ERs were carried out. The three cases I, II, and III had the same target ER = 0.09, and the initial ERs were 0.31, 0.23, and 0.16, respectively. To control variables, these cases were set with the same historical ER decreasing

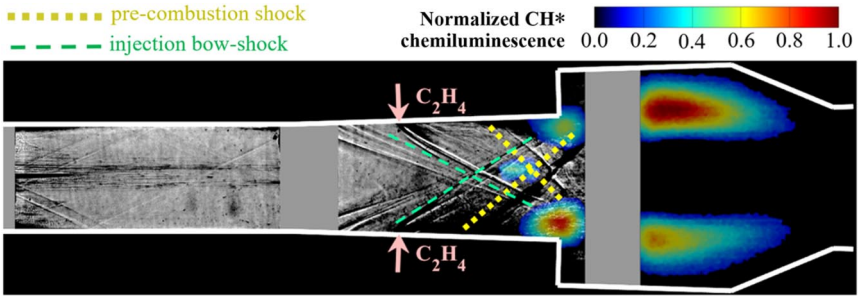


a) The jet-wake stabilized mode at ER=0.09

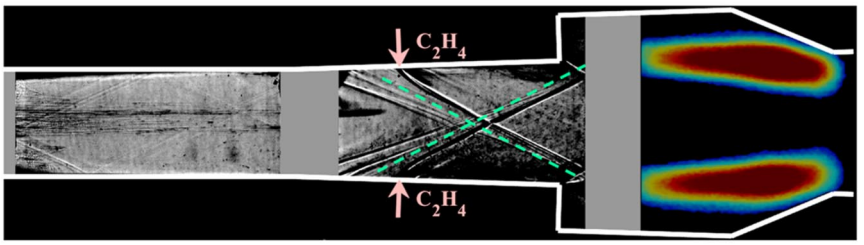


b) The cavity shear-layer stabilized mode at ER=0.09

**Fig. 4 Typical shadowgraph and CH* chemiluminescence pseudocolor images at target ER = 0.09 conditions.**



rate. Because the cavity bottom pressure $p_{cv}$ can represent the cavity-based combustion status, Fig. 5 displays the time histories of $p_{cv}/p_{ref}$ and ER in the three cases. It can be seen that all cases similarly underwent a small pressure catastrophe from 2.9 to 2.4. However, only case I with the highest initial ER of 0.31 underwent another much larger pressure catastrophe from 2.4 to 1.0 subsequently. In the end, significant disparities of $p_{cv}/p_{ref}$ existed between case I and the other two cases, indicating the difference in the final combustion flow states. Similar results were found in repeated tests with the same target ER = 0.10, which were not presented in this paper for simplicity.

States S1, S2, and S3 in Fig. 5 mark the states before and after the two pressure catastrophes, respectively. The pressure catastrophe from states S1 to S2 is much smaller than from S2 to S3. Figure 6 displays typical shadowgraph and CH* chemiluminescence images across the small pressure catastrophe in case I. In each image, $t$ refers to the time axis in Fig. 5. Figure 6 illustrates that the flame sharply weakened across the small catastrophe, but remained in the jet-wake stabilized mode. Moreover, downstream shock movements indicated that flow separation disappeared upstream of the injectors, but separation continued upstream of the cavities. This finding agrees with

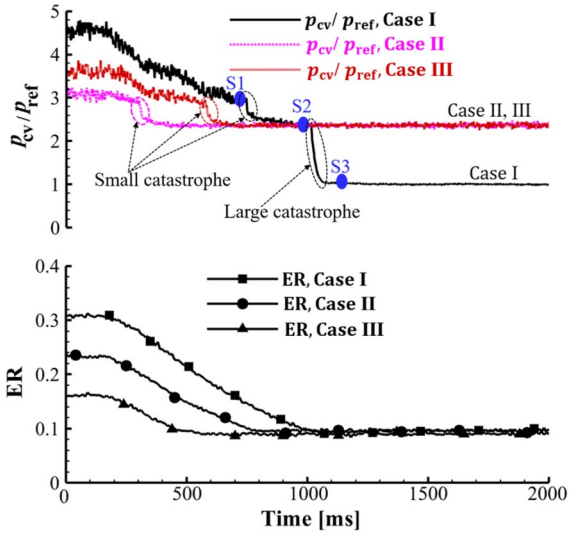


**Fig. 5 Time histories of normalized cavity bottom pressure $p_{cv}/p_{ref}$ and ER in cases I–III.**

that in Fig. 5, in which the decreasing wall pressures remained high enough for separation.

After the small catastrophe, the flame finally remained in the jet-wake stabilized mode in cases II and III. The final combustion flow state is shown in above Fig. 4a. However, another large pressure catastrophe would occur in case I. Figure 7 presents typical shadowgraph and CH* chemiluminescence images across this catastrophe. Figure 7a illustrates that in state S2 before the large catastrophe, the flame and shock structures were similar to the state shown in Fig. 4a. However, differently, case I was not stabilized in this state. As shown in Fig. 7b, the flame moved downstream closer to the cavity aft-walls, along with the downstream shock movement. Then in Fig. 7c, the flame was mostly near the cavity shear layer. Furthermore, the precombustion shock and relevant flow separation disappeared upstream of the cavities. The flame would finally transition to the cavity shear-layer stabilized mode, similar to Fig. 4b.

Moreover, the historical effect of ER decreasing rates on flame stabilizations is presented as follows. To compare with above case I, case IV with a lower ER decreasing rate was arranged. Both cases had the same initial ER of 0.31 and target ER of 0.09. Figure 8 shows the time histories of normalized cavity bottom pressure $p_{cv}/p_{ref}$ and ER in these two cases. The large pressure catastrophe in case I did not appear in case IV, indicating quite different final combustion flow states. For further analysis, Fig. 9 presents typical shadowgraph and CH* chemiluminescence images in case IV. This chart and Fig. 6 demonstrated similar flame/flow evolution features across the small pressure catastrophes in cases I and IV, respectively. However, in contrast, case IV finally remained in the jet-wake stabilized mode as shown in Fig. 9c.

Above all, in the historical ER decreasing path, the initial values and historical decreasing rates of ER regulations mutually affected the flame stabilizations in the dual-solution region. Concretely speaking, if the initial ER was relatively low such as cases II and III, or if the ER decreasing rate was relatively slow such as case IV, then the flame would be finally in the jet-wake stabilized mode as usual. Only if ER decreased rapidly from a very high initial value such as case I, the flame would finally transition to the cavity shear-layer stabilized mode.

### C. Reason Speculations of the ER Regulation Historical Effects on Flame Stabilizations

Section III.B has illustrated the ER regulation historical effects of initial values and decreasing rates on flame stabilizations. This section will speculate the reasons from the view of flow perturbances.

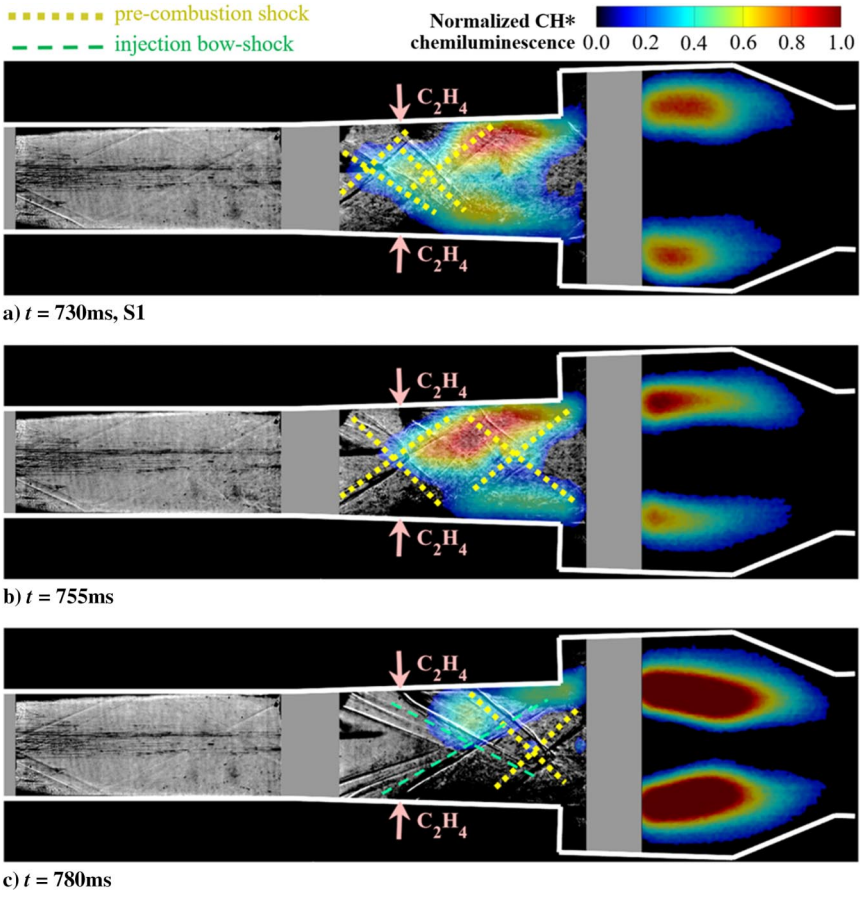


**Fig. 6 Typical shadowgraph and CH* chemiluminescence images across the small pressure catastrophe in case I, where $t$ refers to the time axis in Fig. 5.**

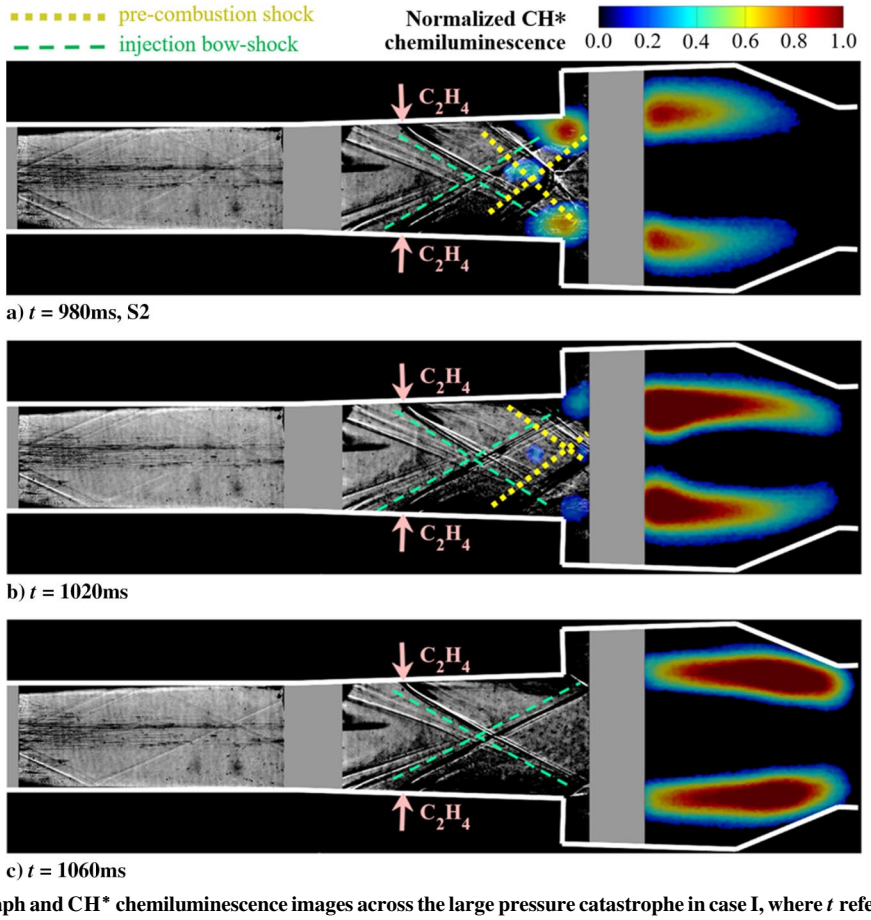


**Fig. 7 Typical shadowgraph and CH* chemiluminescence images across the large pressure catastrophe in case I, where $t$ refers to the time axis in Fig. 5.**

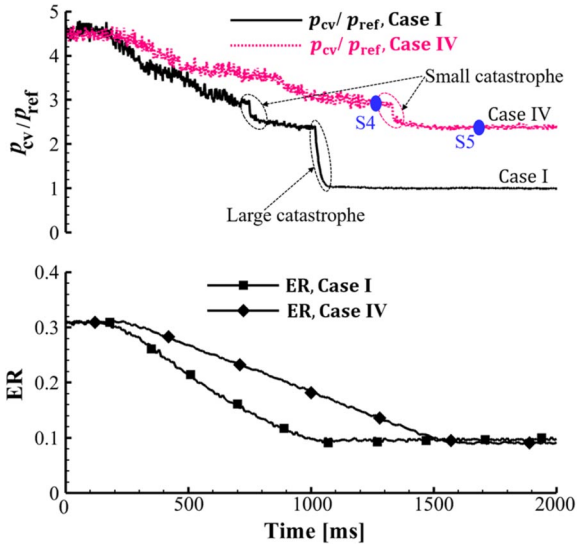


**Fig. 8 Time histories of normalized cavity bottom pressure $p_{cv}/p_{ref}$ and ER in cases I and IV.**

As displayed in Figs. 5–7, decreasing to the same target ER = 0.09, cases II and III remained in the jet-wake stabilized mode. However, case I, with the highest initial ER, finally transitioned to the cavity shear-layer stabilized mode. The possible reason is speculated as below. Theoretically, the minimum backpressure rise $p_m/p_{ref}$ needed for shock/separation is determined by the inflow. An empirical equation is as follows [13]:

$$p_m/p_{ref} = 1 + 0.5\ Ma_{in} \tag{1}$$

$Ma_{in}$ is considered as the test-section inflow of 2.5, and thus $p_m/p_{ref} = 2.3$ by Eq. (1). This is close to $p_{cv}/p_{ref} = 2.4$ in state S2 as shown in above Fig. 5. Figures 5–7 indicate that compared with case I, the flame/shock structural variations from the initial states to state S2 should be relatively small in cases II and III with relatively low initial ERs. The smaller variations probably occurred with smaller flow perturbances, also inferring from the smaller thrust oscillations at lower ERs in above Fig. 4. Consequently, the smaller perturbances could not bring about separation disappearance even when $p_{cv}/p_{ref}$ decreased close to $p_m/p_{ref}$ in cases II and III. The flame could finally remain in the jet-wake stabilized mode. However, in case I, the highest initial ER meant that the initial state had much more intensive flame and stronger separation, together with larger flame/flow oscillations as inferred from Fig. 4. Subsequent flame/shock recessions would be more rapid and should cause much larger flow perturbances. The perturbances were likely to generate backpressures lower than the minimum required for flow separation when ER approached 0.09. Then, separation disappeared, indicating much larger flow speeds that were adverse for combustion. Thus, the flame weakened and finally transitioned to the cavity shear-layer stabilized mode.

The above speculations can be supported by estimations of fuel residence time $\tau_{res}$ and ignition delay time $\tau_{ign}$ as follows. As the flames are commonly near the cavities, the distance from the fuel injectors to the cavity aft-walls is considered as the maximum mixing length $L = 0.16$ m. The inflow speed $u$ is approximately 1200 m/s, and thus $\tau_{res}$ was estimated as $\tau_{res} = L/u = 0.14$ ms. As shown in above Fig. 5, the combustion-zone pressure $p_{cv}$ is 0.75 and 1.8 atm in states S2 and S3, respectively. Considering the $p_{cv}$ values and the target ER of approximately 0.1, Fig. 10 plots $\tau_{ign}$ of ethylene–air premixed gas versus $1000/T$ under the constant pressures by a simplified chemical kinetic model [14]. $T$ represents the incipient gas temperature. This chart illustrates that when $T$ equals the current test inflow temperature $T_{in}$ of 555 K, the ethylene–air mixture cannot

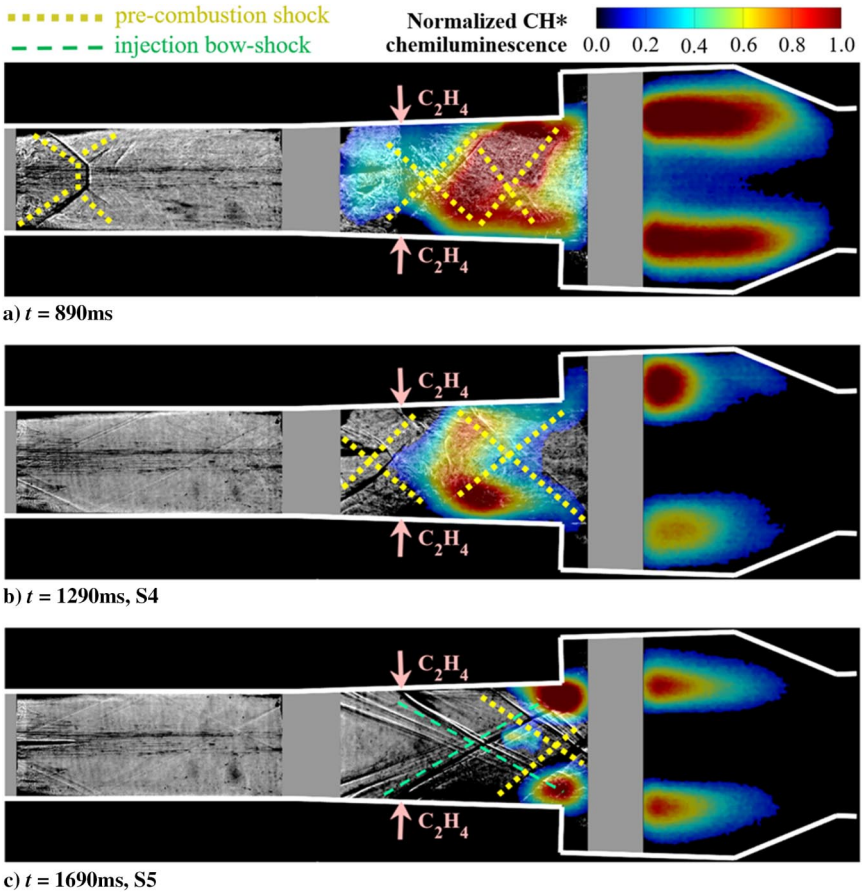


**Fig. 9 Typical shadowgraph and CH* chemiluminescence images in case IV, where $t$ refers to the time axis in Fig. 8.**

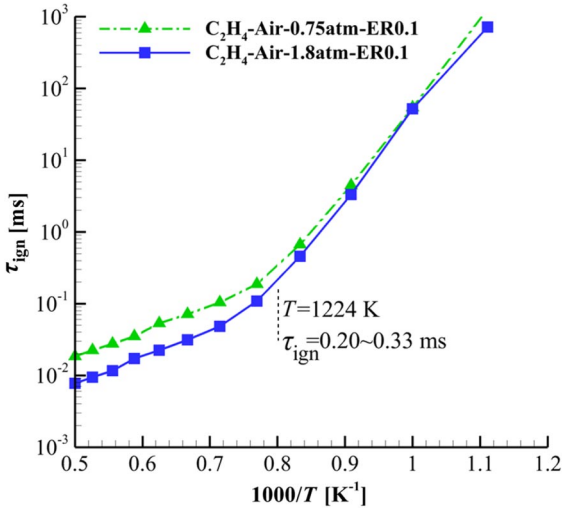


**Fig. 10 Ignition delay time $\tau_{ign}$ vs $1000/T$.**

ignite. Even when $T$ equals the inflow stagnation temperature $T_{in}^{*}$ of 1224 K, $\tau_{ign}$ of approximately 0.20–0.33 ms is just close to $\tau_{res}$ of 0.14 ms, indicating that the flame is still hard to stabilize in the main flow. In other words, flame stabilization in the current test flow relied extremely on the low-speed high-temperature regions of the cavity flame holders. Consequently, across the flame stabilization mode transition in case I, flow separation disappearance upstream of the cavities indicated much higher $\tau_{ign}$. This meant that the flame could not propagate upstream to rebuild flow separation, and thus the transition in case I was irreversible.

Furthermore, the reason for the current finding is speculated from the view of flame/shock-separation interactions. Specifically, a high-enough initial ER meant that the initial jet-wake stabilized flame was sufficiently intensive with large flow separation, and the fast ER decrease in case I meant rapid recessions of flame and separation. When approaching the target ER = 0.09, some originally high-temperature low-speed regions in the main flow rapidly became low-temperature and supersonic, which was adverse for mixing and burning. Then, the originally burning fuel in these regions probably could not mix and burn promptly, indicating an abrupt decrease of heat release. Meanwhile, as the target ER is in the dual-solution region with $p_{cv}$ close to the minimum backpressure required for separation, the lessened heat release probably could no longer maintain separation in the main flow. This manifested as the flame stabilization mode transition shown in Fig. 7. In contrast, in the other cases with lower initial ERs or slower ER decreasing rates, flame/separation recessions were relatively slow enough for timely mixing and burning upstream of the cavities. Thus, the flame could finally remain in the jet-wake stabilized mode.

## IV. Conclusions

To support scramjet engine design and control, this Note experimentally investigated the historical effects of fuel ER regulations on flame stabilizations in a cavity-based scramjet combustor under a Mach 2.5 test inflow. Under the usual historical effects of ER regulation directions, the results illustrated hysteresis associated with dual-solution flame stabilization modes, including the jet-wake stabilization and the cavity shear-layer stabilization. In the dual-solution ER range, the results first demonstrated that initial values and historical decreasing rates of ER regulations also affected flame stabilizations. If ER decreased rapidly from an initially high-enough value, then the flame would unusually transition to the cavity shear-layer stabilized mode. The reason was speculated from the flame/flow evolutions as follows. A high-enough initial ER indicated highly intensive jet-wake stabilized initial flame with large separation. The jet-wake stabilized mode at the target ER in the dual-solution range had backpressures close to the minimum required for separation. More rapid ER decrease meant more rapid flame/separation recessions, which were more likely to generate backpressures that were insufficient for separation at the target ER. Specifically, the more rapid flame/separation recessions meant that some regions in the main flow more rapidly changed from high-temperature low-speed to low-temperature supersonic. The originally burning fuel in these regions probably could not mix and burn timely anymore, indicating abruptly lessened heat release not enough to maintain flow separation. Subsequent separation disappearance in the main flow facilitated the flame stabilization mode transition. Moreover, estimations of ignition delay times proved that flame stabilizations under the current inflow condition strongly relied on cavities' high-temperature low-speed regions. Thus, the transition was irreversible because no separation inhibited flame propagation upstream of the cavities.

## Acknowledgment

This work was supported by the National Natural Science Foundation of China (Grant Nos. U2141220, 11902325 and 11672309).

## References

[1] Zhang, X., Yue, L. J., Huang, T. L., Zhang, Q. F., and Zhang, X. Y., "Numerical Investigation of Mode Transition and Hysteresis in a Cavity-Based Dual-Mode Scramjet Combustor," *Aerospace Science and Technology*, Vol. 94, Nov. 2019, Paper 105420. https://doi.org/10.1016/j.ast.2019.105420

[2] Zhang, X., Zhang, Q. F., Wu, Z. J., Yue, L. J., Gao, Z. B., Luo, W. H., and Chen, H., "Experimental Study of Hysteresis and Catastrophe in a Cavity-Based Scramjet Combustor," *Chinese Journal of Aeronautics*, Sept. 2021. https://doi.org/10.1016/j.cja.2021.08.008

[3] Micka, D. J., and Driscoll, J. F., "Combustion Characteristics of a Dual-Mode Scramjet Combustor with Cavity Flameholder," *Proceedings of the Combustion Institute*, Vol. 32, No. 2, 2009, pp. 2397–2404. https://doi.org/10.1016/j.proci.2008.06.192

[4] Nakaya, S., Kinoshita, R., Lee, J., Ishikawa, H., and Tsue, M., "Analysis of Supersonic Combustion Characteristics of Ethylene/Methane Fuel Mixture on High-Speed Measurements of CH∗ Chemiluminescence," *Proceedings of the Combustion Institute*, Vol. 37, No. 3, 2019, pp. 3749–3756. https://doi.org/10.1016/j.proci.2018.09.011

[5] Tian, Y., Zeng, X. J., Yang, S. H., Xiao, B. G., Zhong, F. Y., and Le, J. L., "Experimental Study on Flame Development and Stabilization in a Kerosene Fueled Supersonic Combustor," *Aerospace Science and Technology*, Vol. 84, Jan. 2019, pp. 510–519. https://doi.org/10.1016/j.ast.2018.10.032

[6] Wang, H. B., Song, X. L., Li, L., Huang, Y. H., and Sun, M. B., "Lean Blowoff Behavior of Cavity-Stabilized Flames in a Supersonic Combustor," *Aerospace Science and Technology*, Vol. 109, Feb. 2021, Paper 106427. https://doi.org/10.1016/j.ast.2020.106427

[7] Rockwell, R. D., Jr., Goyne, C. P., Haw, W., Krauss, R. H., McDaniel, J. C., and Trefny, C. J., "Experimental Study of Test-Medium Vitiation Effects on Dual-Mode Scramjet Performance," *Journal of Propulsion and Power*, Vol. 27, No. 5, 2011, pp. 1135–1142. https://doi.org/10.2514/1.B34180

[8] Wei, B. X., Zhang, Y., Tian, L., Song, G. L., and Xu, X., "Experimental Study on Combustion Mode Transition in an Aero-Ramp Based Scramjet," *48th AIAA/ASME/SAE/ASEE Joint Propulsion Conference & Exhibit*, AIAA Paper 2012-3923, July 2012. https://doi.org/10.2514/6.2012-3923

[9] Bao, W., Yang, Q. C., Chang, J. T., Zong, Y. H., and Hu, J. H., "Dynamic Characteristics of Combustion Mode Transitions in a Strut-Based Scramjet Combustor Model,". *Journal of Propulsion and Power*, Vol. 29, No. 5, 2013, pp. 1244–1248. https://doi.org/10.2514/1.B34921

[10] Zhu, S. H., and Xu, X., "Experimental Study on Mode Transition of the Dual-Mode Scramjet with Two-Staged-Strut Injectors," *Proceedings of the Institution of Mechanical Engineers, Part G: Journal of Aerospace Engineering*, Vol. 232, No. 10, 2018, pp. 1864–1874. https://doi.org/10.1177/0954410017708213

[11] Feng, S., Chang, J. T., Zhang, C. L., Wang, Y. Y., Ma, J. C., and Bao, W., "Experimental and Numerical Investigation on Hysteresis Characteristics and Formation Mechanism for a Variable Geometry Dual-Mode Combustor," *Aerospace Science and Technology*, Vol. 67, Aug. 2017, pp. 96–104. https://doi.org/10.1016/j.ast.2017.03.040

[12] Micka, D. J., "Combustion Stabilization, Structure, and Spreading in a Laboratory Dual-Mode Scramjet Combustor," Ph.D. Dissertation, Univ. of Michigan, Ann Arbor, MI, 2010, p. 40.

[13] Zukoski, E. E., "Turbulent Boundary-Layer Separation in Front of a Forward-Facing Step," *AIAA Journal*, Vol. 5, No. 10, 1967, pp. 1746–1753. https://doi.org/10.2514/3.4299

[14] Petrova, M. V., and Williams, F. A., "A Small Detailed Chemical-Kinetic Mechanism for Hydrocarbon Combustion," *Combustion and Flame*, Vol. 144, No. 3, 2006, pp. 526–544. https://doi.org/10.1016/j.combustflame.2005.07.016

N. D. Sandham
*Associate Editor*